Poly(lactic acid)/polyurethane blend electrospun fibers: structural, thermal, mechanical and surface properties

Sema Samatya Yilmaz[1] · Ayse Aytac[1,2] 🔵

Abstract

Polyurethane (PU)/poly(lactic acid) (PLA) blends having different weight ratios (80:20, 60:40, 50:50, 40:60 and 20:80) were prepared in a suitable solvent environment. A new non-woven fiber surface with a single structure was obtained from the prepared PU/PLA blend solutions by electrospinning method. The effect of different weight ratios on the characteristic properties of PU/PLA fibers was investigated. The obtained electrospun mats were characterized by thermogravimetric analysis (TGA), scanning electron microscopy (SEM), X-ray diffractometry (XRD), differential scanning calorimetry (DSC), Fourier-transform infrared spectroscopy (FTIR), tensile and contact angle tests. The most homogeneous fiber distribution was observed at the structure of 6PU/4PLA (60PU:40PLA w/w) nanofiber. Besides, this fiber was determined to have the highest strength and tensile strain-at-break. Among all fibers, the highest contact angle was observed for 8PU/2PLA (80PU:20PLA w/w) fiber, indicating a hydrophobic structure. According to the DSC results, the melting values of the soft and hard segments of pure PU showed only a melting peak. In XRD results, all electrospun mats which were obtained by blending PLA and PU showed a semi-crystalline structure with low crystallinity. However, these specified fibers showed the thinnest diameter. Thanks to PU/PLA fibers, a new, thinner and more flexible biodegradable surface with perfectly good physical and mechanical properties was obtained. It is expected that the obtained PU/PLA fibers will find a wide range of applications in filtration, liquid-repellent surfaces, medical as wound dressing, and industrial fields.

Keywords PU/PLA blend nanofibers · Electrospinning · Biodegradable · Flexible · Non-woven · Electrospun mats

Introduction

Electrospinning method is a simple yet powerful technique to produce nano/micro-materials [1]. The nanofibers ensure properties like extremely high surface-area-to-volume ratio, porosity, lightness, and resilient mechanical properties [2]. The non-woven nanofibers obtained from polymer solutions by electrospinning have attracted considerable attention, thanks to the inimitable properties of different fields, such as in tissue, and biomedical engineering, nanocomposites, filtration, chemical, food, agriculture, clothing and textiles [3, 4].

Poly(lactic acid) (PLA) which is a biodegradable polyester is obtained from renewable substances, such as potato, corn, and sugar [5]. The recycling of PLA releases no additional carbon dioxide into the atmosphere [6, 7]. Nevertheless, the low toughness property is a disadvantage of PLA. To overcome this negative feature, the PLA is used with plasticizers or it is blended with other polymers as presented in the literature [8]. Thermoplastic polyurethane (TPU) has features like high tensile strength and high elasticity despite low crystallinity and is a polymer belong to the elastomer class. There are two micro-phases in the TPU structure as a soft segment and a hard segment [9, 10]. There are some studies on the use of TPU blend with other polymers, such as thermoplastic polyurethane/polyacrylonitrile, thermoplastic polyurethane/linear poly (ethylene oxide), and thermoplastic polyurethane/poly(vinylidene fluoride) for rechargeable lithium batteries [11–13]. In a study by Jiang et al., they indicated that the PLA may be hardened by elastic poly(butylene adipate-*co*-terephthalate) even though it is a specific rating

✉ Ayse Aytac
aaytac@kocaeli.edu.tr

[1] Polymer Science and Technology Department, Kocaeli University, Kocaeli, Turkey

[2] Chemical Engineering Department, Kocaeli University, Kocaeli, Turkey

of durability and modulus loss [14]. Han and Huang investigated the properties of PLA/TPU blends. According to the result of tensile and Izod impact tests of the mixtures obtained with the melt mixing process, it was observed that by adding TPU to the mixture, the durability of the PLA-based mixtures increases. Also, the globular TPU particles, distributed homogeneously in the PLA matrix, and TPU fragment size increased with increasing TPU amount, and they were determined by morphology analysis [15]. In the study of Feng et al., the PLA/TPU blends have been prepared in different compositions to improve the toughness of PLA and the properties of blends were investigated. It was observed that crack initiation and propagation resistance increased in toughened blends, which were determined by micromechanical analysis [16]. In the Li and Shimuzi study, the toughness of PLA/poly(ether) urethane blends was examined. According to the result of the DMA analysis, it was noticed that these two polymers were partially compatible, in fact, the T_g values of the PLA and TPU phases made them to form a blend. The addition of TPU decreases the rate of crystallization and also the crystallinity of PLA. Besides, it was concluded that the increase in the elongation value and stroke durability by raising the TPU combination in the mixture was the result of the toughening effect of TPU elastomer in PLA [17]. The structural properties of PLA nanofiber scaffolds have been interpreted together with electrospinning process parameters like fiber orientation, winding (collection) speed, and post-thermal operation. The structure of PLA nanofiber was determined by the existence of crystallinity. A cyclic sheet was observed throughout the master axle on the electrospun fiber by an AFM test [18]. Non-porous PLA/monetite electrospun fiber mats were produced by the electrospinning process with suitable conditions. While the electrospinning process of PLA fibers continued, the monetite was obtained as in situ during treatment. There was the ability to change the surfaces of the PLA/monetite electrospun materials with water and heat. By managing the parameters of the electrospinning method, it has been possible to obtain the electrospun webs with the controlled pore region [19]. Huang and Thomas produced the micron-sized electrospun mats with analogous superficial and inner forms from amorphous PLA with the electrospinning method. Thanks to suitable solvent selection which was concluded that both the surface porous structure and the inner porous structure of fiber may be obtained by various methods. It was observed that the choice of chloroform as the solvent in the study created the annular pores limited with 100 nm diameter as superficial. The observed annular pores were produced in humid circumstances with the name of Breath Figure' treatment. It was revealed that assembling chloroform with water-immiscible solvent creates either the surface porous structure (crumple influence)

using a low boiling point solvent, e.g., ethanol or the inner porous structure using a high boiling point solvent, e.g., dimethyl sulfoxide. The PLA fibers that have the porous structure were observed to provide remarkably increased oil absorption ability compared with the electrospun mat surfaces without pore [20]. Lee et al. in their study produced thermoplastic polyurethane elastomer (TPUe) fibers by electrospinning method. To determine the mechanical behavior of TPUe fibers, a series of tensile tests were applied. The TPUe fibers showed the non-linear elastic and non-elastic features that can occur owing to slipping of the hybridized electrospun webs (non-bound or physical bound structure) and fracture of the spun mats in the joints (dot-bound or chemical bound structure)[21]. Lee and Obendorf investigated the behavior of nanofiber surfaces, which prevented the transfer of liquids in preventive clothing structures for agricultural staffs and the stratified cloth structure with polyurethane fiber, which was obtained by electroplating with non-woven textiles on non-woven textiles. It was observed that the completely thin surface of polyurethane fibers significantly improves the preventive structure efficiency for formidable fluids with diversity physicochemical features according to the results of the fluid transition testing. The increase in electrospun fiber mat density decreased the air permeability. Nevertheless, it was concluded that the air permeability of these fibers today is superior to the best preventive clothing surfaces currently available. It was noticed that no remarkable alteration was seen in the humidity vapor transfer of nanofiber obtained by the electrospinning method. The pore dimension dispersion evaluations demonstrated the compatibility of engineering pore dimension with the amount of fibers area volume. So, it was concluded that the grade of preservation and thermal comfort of layered fabric structure can be controlled [22].

In this study, the aim is to fabricate electrospun fiber mats from PU/PLA blends with electrospinning process as one of the manufacturing techniques guaranteed by nanotechnology, against the traditional production methods in most fields (extrusion, solution casting, etc.) for surface production of PU/PLA blends. According to the author's knowledge, there is no study in the literature investigating the properties of PU/PLA mixtures in different compositions by electrospinning. In the study, the production of non-woven surfaces with the aim of electrospinning method from different weight ratios of PU/PLA blend solutions has been achieved. The characterization studies of the obtained nanofibers have been reported. It has been observed that the idea of areas for the use of PU/PLA electrospun non-woven felts is obtained through characterization tests. The use of PU/PLA nanofiber products is thought to have wide applications in areas where there is a limited choice of suitable materials.

Experimental

Materials

For these studies, Estane® GP52DTNAT055 which was provided from Lubrizol (Velox) was used as aromatic pol-yether-based thermoplastic polyurethane. Also, biodegrad-able 4043D poly(lactic) acid that has a molecular weight of 120,000 g/mol was supplied from Nature Works. Dimeth-ylformamide (DMF) and chloroform (CF) solvents were purchased from Merck.

Methods

Solution preparation

The PLA and PU pellets were placed in a furnace at 80 °C for 12 h to remove the moisture on the PLA and PU pellets. Then, pure PLA and PU solutions were prepared and all PU/PLA blends were turned into the solution at 5 different ratios. The PLA was homogeneously dissolved in a mixture of CF and DMF at an 80:20 weight ratio with stirring at room temperature for 4 h. The 10% (by wt) pure PLA solu-tion was treated with the electrospinning process.

PU was dissolved in much the same way as PLA dissolu-tion. Differently, after 4 h of stirring at room temperature, it was stirred for 30 min with heating at 120 °C. The pure PU solution of 10% (by wt) concentration was completely homogeneously dissolved and it was treated by the electro-spinning method. The PU/PLA blends were prepared for 80, 60, 50, 40 and 20% ratios. The sample codes of the prepared surfaces were called 8PU2PLA, 6PU4PLA, 5PU5PLA, 4PU6PLA and 2PU8PLA. All PU/PLA mixtures were simultaneously created as a solution in a beaker. The PU/PLA blends were prepared like pure PU solution. Hence, PU/PLA solutions were realized exactly in the dissolution process to obtain a homogeneous mixture. The 10% (by wt) PU/PLA solutions, obtained with different compositions, were used for the electrospinning process.The conductiv-ity of the solvents was measured with a liquid conductivity meter at room temperature (24 °C). It was determined as 0.4 μS/cm for DMF and 0.0 μS/cm for CF.

Electrospinning treatment

All the obtained solutions were used in the electrospin-ning process out of delay. The electrospinning process was applied initially to pure PLA and pure PU solutions. While electrospinning operation of both pure PLA and pure PU was realized with requirements of 0.5 mL/h feeding speed, 20 cm distance and 15 kV supplied voltage, it was performed with 0.5 mL/h feed rate, 20 cm distance and 18 kV applied voltage for PU/PLA blends. For the electrospinning method, a blunt syringe end having a dimension of 0.91 mm (20G gage/inch) was used conveniently for 10% (by wt) solution concentration. The electrospinning processes were per-formed at room temperature (24 °C ± 2) and the relative moisture content was 65%.

Characterization

The surface images of the electrospun mats were displayed with a scanning electron microscope named QUANTA 400F Field Emission in this study. The chemical structure of fibers was determined with IR spectra in the interval of 500–4000 cm^{-1} on a Perkin Elmer spectrum 100 FTIR device with ATR unit. Thermogravimetric analysis (TGA) of the fibers was conducted with Mettler Toledo TGA 1 in the interval of 25–600 °C, with a heating rate of 10 °C/min and high-purity nitrogen gas which was sent to the process with a flux rate of 50 mL/min. The thermal properties of fibers including glass transition temperature (T_g), melting temperature (T_m), heat of fusion (ΔH_{matrix}), and degree of crystallinity (X_c) were determined using a Mettler Toledo DSC 1 branded appliance. The differential scanning calo-rimetry (DSC) analysis of fibers was carried out in a one-stage step with a temperature interval of (-50)–300 °C and a heating rate of 10 °C/min, and the high-purity nitrogen gas was sent to the process at a flux rate of 50 mL/min during measurements. The degree of crystallinity (X_c) of fibers was calculated using the (ΔH_m^0) value of PLA from the results of the DSC analysis with the following equation. The (ΔH_m^0) value of PLA was used as 93.7 J/g obtained from previous studies [23].

$$Xc(\%\text{crystallinity}) = \frac{\Delta H_m - \Delta H_c}{(\omega_f) \times \Delta H_m^0} \qquad (1)$$

where ΔH_m is the heat of melting of each sample, ΔH_c is the crystallization enthalpy, ω_f is the weight fraction, and ΔH_m^0 is the heat of melting of the matrix.

The wettability properties of fibers were determined using the hanging droplet method with an Attension Theta Lite device at room temperature (24 °C ± 2 °C). With this method, the static contact angle measurement was per-formed. Distilled water droplets in the amount of 10 μL were dropped onto a surface. The water drop was visualized in the computer environment through a camera equipped with a powerful optical lens. The tangent value of the drop contact angle was calculated with a computer software. The water repellency test was concluded by calculating the aver-age of the angle values recorded for 9 s with the camera. In this way, each nanofiber sample was tested 10 times. The mechanical properties analysis of fibers was carried out on

a pulling device (Lloyd Instruments LRX Plus) running at 1/10 mm/min pulling speed, at 5 kN load, at room temperature (24 °C ± 2 °C) and under the conditions of ASTM D882 standard. In tensile test, the fibers were prepared at dimensions of 50 mm × 15 mm and the mean thickness value of 0.20 mm. The tensile test processes were applied to all fibers 5 times and the average of obtained values was reported. Besides, a Rigaku Ultima-IV branded XRD device was used for XRD analysis of fibers in this study.

Flow times of pure solvents and solvent mixture (80:20 CF/DMF w/w) were measured for the determination of relative viscosity. Then, 1% concentration solutions of pure PU, pure PLA and PU/PLA blend polymers were prepared. Flow time measurement of each solution was carried out with an Ubbelohde (Koehler) at room temperature (24 °C). The relative viscosity (η_r) of pure PU, pure PLA, and PU/PLA blend solutions was calculated from the results of the

flow time measurement with the Ubbelohde using the following equation:

$$\eta_r = \frac{\eta}{\eta_0} = \frac{t}{t_0} \tag{2}$$

where η is the viscosity of the solution, η_0 is the solvent viscosity, η_r is the relative viscosity, t is the flow time of the solution and t_0 is the solvent flow time.

Results and discussion

Surface micrograph (SEM)

SEM micrographs of the obtained all fibers are given in Fig. 1. The surface images of all nanofibers except for
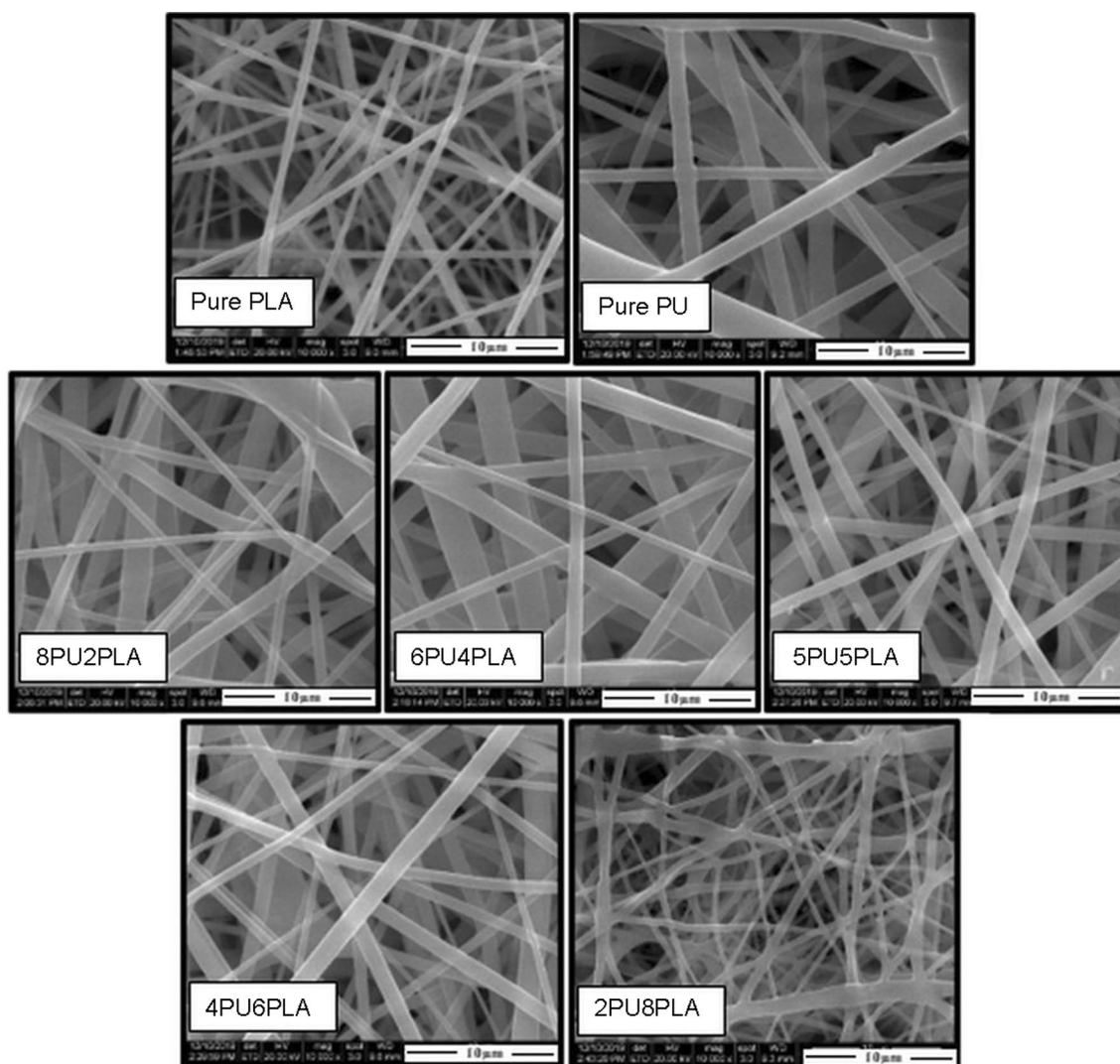

Fig. 1 Surface images of electrospun fibers

Table 1 Flow time and relative viscosity values of samples

Sample	Flow time (s)	η_r
CF	7.1	–
DMF	10.1	–
8CF/2DMF	8.3	–
PLA	11.6	1.4
PU	27.3	3.3
8PU2PLA	25.2	3.0
6PU4PLA	21.4	2.6
5PU5PLA	18.9	2.3
4PU6PLA	16.2	2.0
2PU8PLA	14.2	1.7

Fig. 2 Average fiber diameter (nm) of electrospun fibers

2PU8PLA nanofiber are beadless, smooth, and homogeneous. However, the branching was observed for 2PU8PLA nanofiber in the SEM micrographs. Because of viscosity due to molecular weight which is not optimal for constant process conditions, fiber formation can also create adherent, beaded and irregular fiber structures (Table 1). In the 2PU8PLA nanofiber, it can be thought that the stress applied during the process as a result of the polymer surface tension, which may have changed due to the interaction between PU and PLA, is not sufficient in fiber formation. It can also be thought that another reason for the cohesive fibers may be caused by moisture content [24]. Schiffman et al. reported that the branching on the fibers was due to different percentages of moisture during processing [24]. They described that the branched fibers were obtained in the 20–25% moisture content while the non-branched fibers were created when the moisture content was twice as high as 40–45%. In this study, in all nanofiber productions, the syringe and the collector distance, the amount of tension applied and the solution concentration were the same. Therefore, the formation of adhered and branched fibers may be little affected by the difference in moisture content in the 2PU8PLA solution compared to solutions of other nanofibers.

Along with SEM micrographs, the mean diameter of all the fibers was also measured. The graph of the average diameter length of all nanofibers is given in Fig. 2. The average diameter of pure PLA fibers and pure PU fibers, respectively, were the values of 330 nm and 1025 nm. Pure PU nanofibers were obtained as about 3 times thicker than pure PLA nanofibers. The closest diameter to pure PLA nanofibers was the 2PU8PLA nanofiber sample with an average of 383 nm. In this study, the presence of PLA has an effect on reducing the diameter values of electrospun fiber diameter values and the presence of PU has shown an effect on reducing the diameter values of electrospun mat. Besides, a reverse proportion correlation has been seen between the 8PU2PLA and 6PU4PLA electrospun fiber mats, where the quantity of PU is higher than the quantity of PLA until the amount of PLA is balanced as equal. In diameter measurement, the
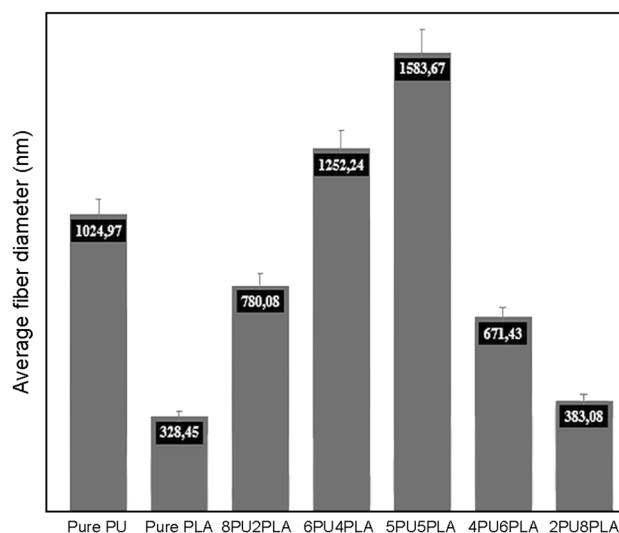
5PLA5PU electrospun web was observed as the thickest fiber. Therewithal, the closest diameter of the 6PU4PLA fiber network was seen in the 5PU5PLA fiber network. The 4PU6PLA and 2PU8PLA fiber mats were reported to have the thinnest diameter in this study.

Regarding all the electrospun mats that were obtained in the same electrospinning operation conditions, the determinant factor that straightly influenced the fiber thinness modification was accepted as the difference of polymer structure. As the weight ratios of the solutions prepared to form fibers changed, the diameter of the fibers spun by electrospinning also changed. In previous studies [25, 26], the fiber diameter modification associated with the irregular distribution of load and decreased or increased molecular weight of the structure were reported. The irregular distribution of load can enable the electrostatic thrust forces to acquire over the surface tension in several areas more easily. At the same time, both the low viscosity of the polymer and the low molecular weight of the polymer can provide faster splitting of the electrospinning jet. Even though the concentrations of pure PU solution and pure PLA solution prepared in this study are the same, the molecular weight of pure PU polymer used in this study is higher than that of pure PLA polymer, but the viscosities of these polymers are dissimilar from each other. Increasing the viscosity in the electrospinning process has affected the fiber diameter to increase. Since the molecular weight of PLA is lower, thinner fibers have been obtained.

The fiber fineness expected in this study is the values between pure PU and pure PLA nanofibers. Except for 5PU5PLA and 6PU4PLA nanofibers, other fibers produced fiber fineness within the expected ranges. The relative viscosity measurements of the solutions affecting fiber

diameters and fiber irregularity are shown in Table 1. Viscosity is evaluated in direct proportion to molecular weight. In this case, it was thought that as the amount of PU in the PU/PLA mixture increased, the viscosity increased and thus its molecular weight increased. It is seen from the increase in fiber fineness that the molecular weights of the blended nanofibers increased compared to that of pure PLA. It was observed that the molecular weight of 5PU5PLA and 6PU4PLA nanofibers increased and each had favorable viscosity for constant electrospinning conditions, resulting in thicker but not adherent fibers than pure nanofibers. In addition, as a biodegradable nanomaterial, having a balanced mixture with a higher PLA ratio would be beneficial in terms of production.

Fourier-transform infrared spectroscopy (FTIR)

The FTIR-ATR spectra of the electrospun nanofiber mats are given in Fig. 3. The characteristic peak of PU is 1600 cm^{-1} and belongs to aromatic C=O group oscillations. Other peaks of pure PU fiber were observed for N–H group vibration at 3318 cm^{-1}, for CH$_2$ at 2855 cm^{-1}, for C=O group vibrations at 1709 cm^{-1} and vibrations (N–H) + (C–N) + (C–H) at 1311 cm^{-1} [27]. While the peak of 1600 cm^{-1} was not observed at pure PLA fiber, this peak was seen at PU/PLA nanofiber mats. The characteristic peak of PLA was C=O stress vibration at 1753 cm^{-1}. In addition, other peaks of pure PLA fiber are seen for CH$_3$ at 1452 cm^{-1} and for CH$_3$ at 1366 cm^{-1}. The peak at 1753 cm^{-1} was seen for PLA/PU electrospun webs while this peak was not observed for pure PU fiber. The FTIR spectra showed the peaks of carbonyl group (C–O–C) at 1260 cm^{-1}, (C–O–H) vibrations at 1088 cm^{-1} and CH$_2$ tensile vibration at 2932 cm^{-1}. The

increase in the peak at 3318 cm^{-1} was seen in all PU/PLA nanofiber FTIR spectra, which can be interpreted as increasing the number of hydrogen bonds formed between the soft and hard parts of the urethane phase mixture [28]. Besides, DMF and CF solvents were found to be removed from the structure of the fibers by electrospinning, because the characteristic peaks of the solvents were not seen in the FTIR analysis.

Thermogravimetric analysis (TGA)

The TGA decomposition temperature values of all fibers are given in Table 2. Thermal decomposition of pure PU fiber has emerged three necks in the temperatures near 297 °C, 352 °C and 420 °C. This three-stage decomposition is due to distinct deterioration actions of urethane bonds in the soft part and polyol groups in the hard part of PU. Pure PU fiber left a residue of 8.82%. Based on TGA analysis, the T_{max} temperature for pure PLA fiber was observed at 354 °C with 3.71% residue.

The TGA decomposition curves of all the fiber mats are shown in Fig. 4. With the participation of PU in the structure of another nanofiber, it was observed that the initial weight degradation temperatures begin to drop and that the decomposition temperatures follow a temperature below the decomposition temperature of PLA compared to that of pure PLA.

Therewithal, all blended fibers gave three-neck curves. It was observed that the degradation temperature of 5% (T_{deg5}) for pure PLA nanofiber was higher than that for pure PU nanofiber. The results were obtained in the value range of these two nanofibers for blended fibers. When the PU/PLA fibers were examined, it was seen that the decomposition curve of 8PU2PLA nanofiber was closest to the pure PU decomposition curve. It has been observed that the 2PU8PLA and 6PU4PLA nanofibers show a value lower than the T_{dg5} value of the other blended and pure nanofibers. The lowest amount of residue was observed in these two fibers. The temperature at which it started to decompose
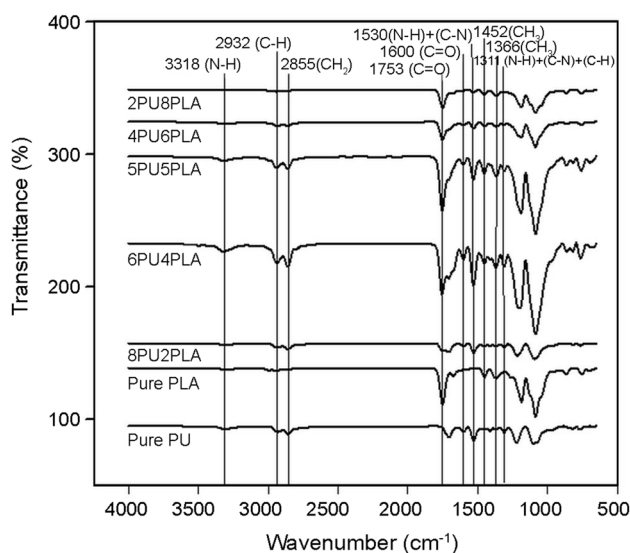

Fig. 3 FTIR spectra of electrospun fibers

Table 2 TGA decomposition values of electrospun fibers

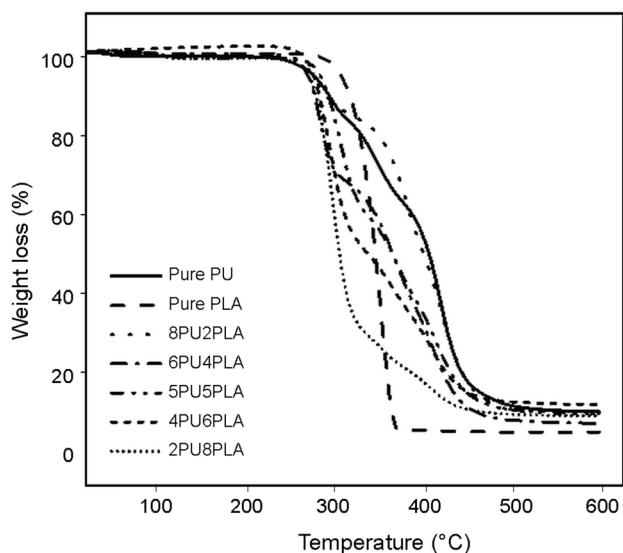| Sample	T_{max} (°C)			T_{deg5} (°C)	Residue 600 °C (% by wt)
	1.st step	2.nd step	3.rd step		
Pure PLA	354.65	–	–	307.01	3.71
Pure PU	297.19	352.13	420.08	274.54	8.82
8PU2PLA	283.35	381.49	420.92	274.96	8.31
6PU4PLA	285.87	368.49	412.11	272.03	5.88
5PU5PLA	308.10	372.26	414.62	284.19	8.51
4PU6PLA	296.35	366.81	410.43	277.90	10.66
2PU8PLA	300.55	356.33	408.33	271.19	7.81

Fig. 4 TGA decomposition curves of electrospun fibers

Fig. 5 DSC curves of electrospun fibers

was the highest in these two fibers compared to other fibers. However, only 2PU8PLA nanofiber showed the lowest temperatures in the 2nd and 3rd necks. These necks are due to the differences in the distribution of hard and soft parts in polyurethane. As the distribution of these regions within the structure changed, the thermal properties of the fiber also changed. The residual amount was higher in pure PU. This residual amount in PU/PLA blend fibers is thought to belong to the hard parts and the structures bonded to the hard parts.

Differential scanning calorimetry (DSC)

The T_g value of pure PLA nanofibers is 59 °C and the T_m temperature is 154 °C. The T_g value of pure PU was found as -40 °C and two different T_m values were seen at 30 °C and 110 °C for the soft and hard parts of PU, respectively [29]. The DSC graphs of all fibers are given in Fig. 5. The crystallization and fusion temperatures of the diisocyanate or hard sections of TPU have been associated with the kind of polyol or soft sections and the mean series length of the crystallizable elements [30]. Since the soft parts are the characteristic structure of the TPU polymer, the soft parts in the TPU give negative values of T_g since they were not determined or disappeared completely in PU/PLA electrospun mats. PU/PLA nanofibers gave the T_g value of pure PLA as a second T_g between 59 °C and 61 °C. While the temperature of the hard segment was not observed on the PU/PLA electrospun mats, the melting temperature values of the soft and hard sections of PU gave one fusion top by observing a slip in all nanofibers blended with PLA at temperature values around 150 °C.

The harmony of polymer mixtures may be defined by the deflection of T_g values of the constituents that form the blend from th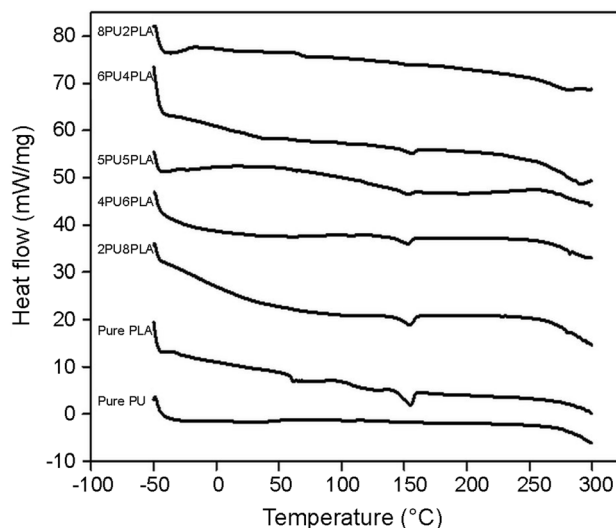e characteristic values of the polymers in it and are closer to each other. However, the presence of T_g of the soft parts of PU provides flexibility in blended nanofibers. In the absence of T_g in the soft parts, it can be said that these parts exactly appear and mixed as a hard part in the structure. The presence of soft parts in the PU structure that cause loss of PLA stiffness with the values obtained from the DSC curves is shown in Table 3.

According to the enthalpy values obtained from the DSC graphs, 8PU2PLA, 6PU4PLA with 5PU5PLA and 4PU6PLA with 2PU8PLA were seen to have close percentage values of crystallinity. While 4PU6PLA and 2PU8PLA nanofibers were higher than pure PLA, 8PU2PLA, 6PU4PLA, and 5PU5PLA nanofibers showed lower values than pure PLA. The highest crystallinity ratios were observed in nanofiber that had high PLA content. Crystallization also decreased in electrospun non-woven mats by decreasing the presence of PLA and increasing the presence of PU in the structure. At the same time, it was observed that the highest crystallization rate among electrospun non-woven mats with high PU presence was 6PLA4PU fiber for 16.46%. 100% crystalline fusion enthalpy of PU was not observed and the crystallinity was not calculated for the pure PU electrospun mat in DSC.

Wettability properties

When the surface water affinities of all the electrospun mats were examined in Fig. 6, it was found that pure PU, pure PLA, and 8PU2PLA nanofibers were more hydrophobic than other nanofibers with $120° \pm 2$ contact angle value. When the other nanofibers were evaluated, it was noted that the contact angle of $101° \pm 5$ showed a hydrophobic property with the values close to each other but lower than the contact angle values of pure PLA, pure PU, and 8PU2PLA electrospun
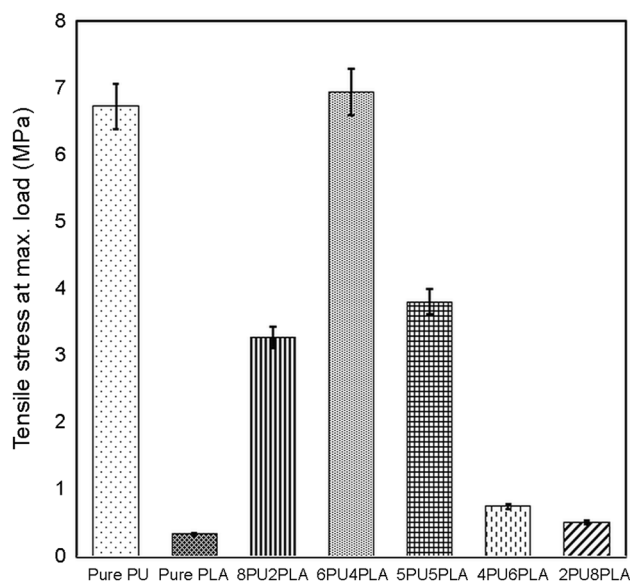
Table 3 Different properties determined from DSC curves of electrospun fibers

Samples	T_g (°C)		T_m (°C)		ΔH_m (Jg^{-1})		% X_c of PLA
Pure PLA	59		154		19.98		21.32
Pure PU	− 49		30 soft part	110 hard part	10,25 soft part	0,49 hard part	–
8PU2PLA	− 14 (PU)	65 (PLA)	153		2.58		13.76
6PU4PLA	− 30 (PU)	61 (PLA)	155		6.17		16.46
5PU5PLA	− 26 (PU)	61 (PLA)	152		6.10		13.02
4PU6PLA	59		153		15.04		26.75
2PU8PLA	–		154		17.74		23.66
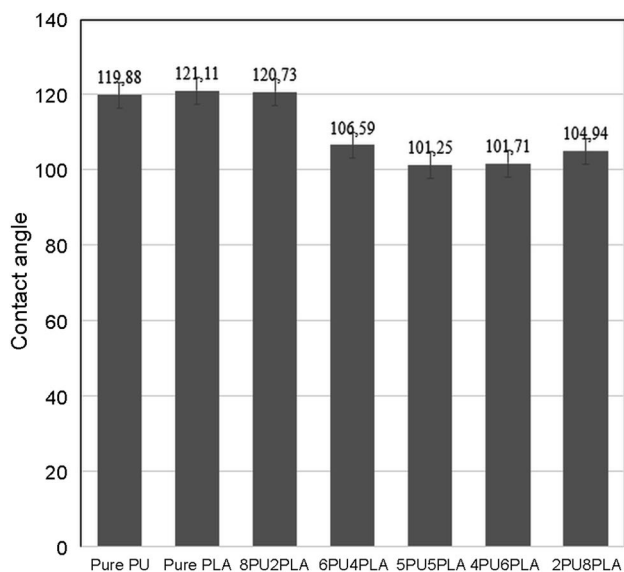
Fig. 6 Comparison of water repellent properties of electrospun fibers

Fig. 7 Tensile stress at maximum load (MPa) of electrospun fibers

mats. In another remarkable point, the 2PU8PLA nanofiber sample was expected to give a value between $120° \pm 2$ contact angle values of pure PLA and pure PU nanofiber, just like 8PU2PLA nanofiber. However, the 2PU8PLA nanofiber sample showed an angle of 104°. So, a comment can be made as follows: although the contact angle value of pure PLA was higher than that of pure PU, when the amount of PU in the blend samples was high, it could be interpreted that the water repellency could have increased significantly. When the amount of PLA was high, it could be said that the contact angle values were at a low level since the bond structures that showed water repellency feature were low.

Due to the fact that 8PU2PLA fiber has the highest hydrophobicity of mixed fibers in contact angle measurement, so according to the DSC results, a relationship can be established between crystallization in its structure and hydrophobicity. In the Lostocco study, it was emphasized that the hydrolysis of amorphous and crystallized poly(lactic acid)/poly(hexamethylene succinate) mixtures had a significant effect on the degradation delay in regular crystalline phases

as well as the hydrophobicity of poly (hexamethylene succinate) [31].

Mechanical properties

The results of tensile stress at maximum load (MPa), tensile strain at maximum load (%), and tensile strain-at-break (%) of fibers, obtained from the mechanical analysis, are shown in Figs. 7, 8 and 9, respectively. When the maximum tensile stress graphs given in Fig. 7 were examined, it was observed that the tensile stress of the pure PU electrospun mat and 6PU4PLA electrospun mat showed the maximum values which were almost equal to each other. While the hard sections of pure PU fiber increased the tensile stress, its soft sections increased the extension in the structure. The structure of pure PLA electrospun mat demonstrates physical properties like brittle and weak. However, PLA strength and elongation were found to be low compared to other physical states such as
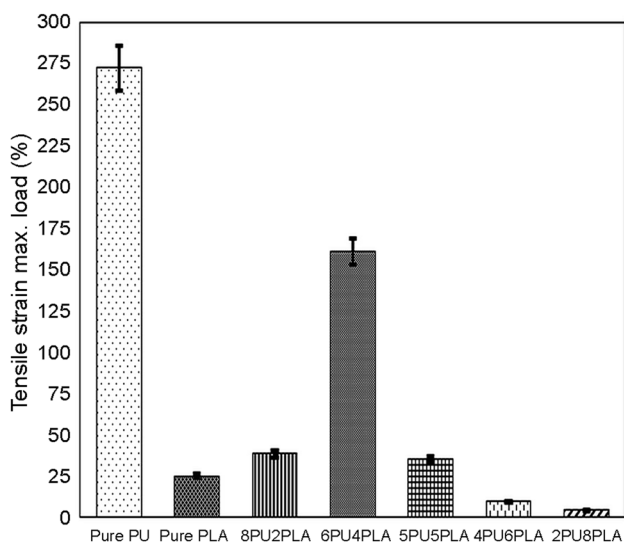
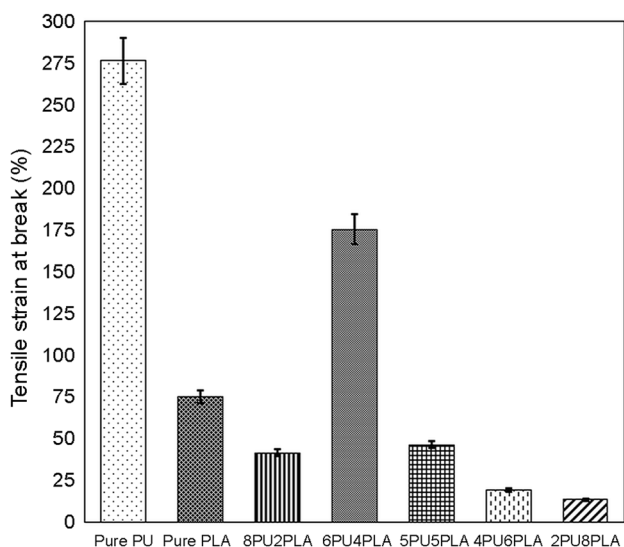**Fig. 8** Tensile strain at maximum load (%) of electrospun fibers

Fig. 9 Tensile strain-at-break (%) of electrospun fibers

Comparing to the durability value of pure PLA when PU was incorporated into the structure, it was observed that the PU decreased brittleness in the structure of PLA and at the same time supplied the improvement of the resistance and stiffness. In the maximum tensile stress graphs, there was a linear increment in the tensile durability with increasing PU quantity among electrospun mats. It was noticed that incremental PU amount did not increase the durability value of PU/PLA electrospun mats linearly.

So much so that the strength of the 6PU4PLA nanofiber has been higher than that of 8PU2PLA nanofiber. Therefore, it can be said that the most optimum blend weight ratio for the improvement of the strength value among the blends is related to 6PU4PLA, so for future studies depending on the end use areas, the tensile test results would be important according to the strength values. Since fiber and fibrous surfaces do not show flowing behavior, tensile strain at the maximum load and strain-at-break values are almost the same and these graphics can be evaluated together. When the tensile strain at the maximum load (%) in Fig. 8 and strain-at-break (%) in Fig. 9 are evaluated together, the value of tensile strain at the maximum load and tensile strain-at-break of pure PU electrospun mats would be close to each other, and approximately is drawn 4.5 times their original length. The flexibility feature that is provided by soft parts of the PU was also observed in the pure PU electrospun mats. Pure PLA electrospun mat showed significantly less extension value than pure PU electrospun mat.

It has been interpreted that the high rupture value of the pure PLA electrospun mat seen at the graph of tensile strain-at-break in Fig. 9 is due to each leaving one by one from the electrospun webs after rupture during the tensile test. This is a behavior that can be ignored on the nanofiber and fiber surfaces. Because as soon as the fiber breaks and the strength starts to decrease, in all fiber materials with fiber network, the fibers can continue to break wire by wire and separately. Therefore, the value of strain-at-break continues until the last wire holding the rest is broken. However, it can be said that for nanofiber or fibrous structures it is not meaningful that the strain-at-break is greater than the tensile strain at the maximum load. When the extension results of the 6PU4PLA electrospun mat were evaluated, it was decided that this fiber is the most similar structure to the pure PU electrospun mat. Elongation behaviors of other blended fibers were found to be quite low, close to or lower than those of pure PLA. At the same time, it can be interpreted that this nanofiber with the highest strength and elongation behavior values for the 6PU4PLA sample has the optimum weight ratio value.

X-ray diffraction (XRD)

In Fig. 10, the XRD graphics describing the crystallinity properties of all fibers are compared. PU/PLA fibers

film, according to the tensile test results of pure PLA film structures [32]. This information is correct from the results of nanofiber structures.

As the PLA value in the structure of the nanofibers increases, the strength values decrease and it approaches the strength value of the pure PLA. Especially, the strength values of 4PU6PLA and 2PU8PLA nanofibers were very low. By an incremental quantity of PU incorporated into the structure, it was observed that 8PU2PLA and 5PU5PLA electrospun mats were upward of the durability value of the pure PLA electrospun mat. In addition, among the resistance values of pure PU and pure PLA electrospun mats, these fibers have shown the closest values.
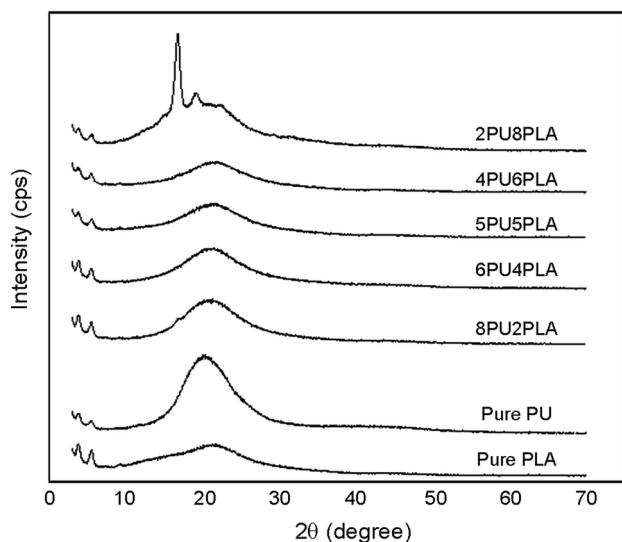
Fig. 10 XRD graphs of pure PLA, pure PU and PLA/PU nanofibers

displayed a wide diffraction peak at $2\theta = 21.00°$ (± 0.7) (diffraction peak due to PU soft segment and PLA) along with a minor hill at $2\theta = 16.77°$ (± 0.2) (diffraction peak because of PLA), demonstrating its amorphous structure [28]. PU/PLA polymer blends are thermodynamically a miscible blend and prevent the generation of single-crystalline stages [33, 34].

The sharp and wide peak at $2\theta = 19.88°$ is assigned to the pure PU nanofibers, indicating a typical XRD pattern with a low degree of crystallinity. It is shown in the literature that the degree of crystallinity of PU is controlled by the ratio of pre-polymer and polyol. The pure PU that has the pre-polymer and polyol mass ratio of 1/1 is more crystalline (37% crystallinity), with the densest peaks determined at $2\theta = 11°$ and $2\theta = 19°$ [35]. Since pure PLA nanofibers showed $2\theta = 14.2°$ and $2\theta = 21.44°$, wide but short-wavelength peaks were observed for them, and also they showed a lower crystallinity than pure PU fibers. According to the XRD patterns, other blended nanofibers except 2PU8PLA nanofiber showed peaks at 2θ values approximately similar to 2θ value of pure PLA, and that they exhibited a percentage crystallinity value between that of pure PLA and PU that has as low semi-crystal structure. However, the sharp peaks at $2\theta = 14.97°$, $2\theta = 16.77°$, $2\theta = 19.17°$ and $2\theta = 22.14°$ observed for the fiber of 2PU8PLA indicate the increased crystallinity in the fiber structure. The XRD results indicate that the crystallinity of pure PU fiber could not be determined by DSC analysis. It has been determined that all electrospun mats obtained by blending semi-crystalline pure PLA and PU have a semi-crystalline structure. In DSC analysis, the 4PU6PLA and 2PU8PLA fibers showed the highest percentage of crystallinity as compared to the other blends compositions, and the T_m value of each blend fiber was found. Thus, both DSC and XRD analyses determined

that the nanomaterials obtained have a semi-crystalline structure with a low crystal content.

Conclusion

The electrospun mats from PU/PLA mixtures were successfully produced using an electrospinning method and the characterization tests of electrospun fibers were carried out in this research. The SEM images showed that all electrospun mats except 2PU8PLA fiber have a very regular, quite smooth, homogeneous, and beadless structure. The 6PU4PLA electrospun fiber indicated the smoothest surface property. However, in the mechanical tests, the 6PU4PLA electrospun mat displayed the highest durability and tensile strain-at-break. According to the diameter measurements by the SEM, the thinnest diameter was observed for 4PU6PLA and 2PU8PLA samples and the 5PLA5PU electrospun mat was determined being the thickest electrospun non-woven material with approximately 1500 nm diameter. The strength and elongation of 5PLA5PU and 8PU2PLA samples were close to those of 6PU4PLA nanofiber. According to the DSC results, 23% 2PU8PLA and 26.75% 4PU6PLA displayed the highest crystallinity. Also, all electrospun mats obtained by blending semi-crystalline pure PLA and PU exhibited percentage crystallinity values between those of pure PLA and PU with a low semi-crystal structure. Besides, a hydrophobic surface structure was observed generally in all prepared fibers. Compared to other nanofibers, 8PU2PLA fiber showed hydrophobic property with the highest angle. A curve at the average values of both pure PLA and pure PU temperatures in TGA was obtained for 8PU2PLA fiber. When thermal properties were examined, the fusion values of the soft and hard segments of PU displayed only a melting peak around 150 °C such as pure PLA in all the electrospun mats. As a result, all blended nanofibers showed significant results in different analyses. It can be said that there is a harmonious interaction between these blended fibers. Further studies can identify more uses for PU/PLA non-woven mats using more advanced experiments.

References

1. Huang ZM, Zhang YZ, Kotaki M, Ramakrishna S (2003) A review on polymer nanofibers by electrospinning and their applications in nanocomposites. Compos Sci Technol 63:2223–2253
2. Tijing LD, Ruelo MTG, Amarjargal A, Pant HR, Park CH, Kim DW, Kim CS (2012) Antibacterial and superhydrophilic electrospun polyurethane nanocomposites fibers containing tourmaline nanoparticles. Chem Eng J 197:41–48
3. Shi Q, Vitchuli N, Nowak J, Noar J, Caldwell JM, Breidt F, Bourham M, McCord M, Zhang XW (2011) One-step synthesis of silver nanoparticle-filled nylon 6 nanofibers and their antibacterial properties. J Mater Chem 21:10330–10335

4. Nataraj S, Yang K (2012) Polyacrylonitrile-based nanofibers A state of the art review. Polym Sci 37:487–513

5. Auras R, Harte B, Selke S (2004) An overview of polylactides as packaging materials. Macromol Biosci 4:835–864

6. Vink ET, Rabago KR, Glassner DA, Gruber PR (2003) Applications of life cycle assessment to NatureWorksTM polylactide (PLA) production. Polym Degrad Stabil 80:403–419

7. Vink ET, Rábago K, Glassner DA, Springs B, Q'Connor RP, Kolstad J (2004) The sustainability of NatureworksTM polylactide polymers and IngeoTM polylactide fibersa: an update of the future. Macromol Biosci 4:551–564

8. Hazer S, Çoban M, Aytaç A (2018) A study on carbon fiber reinforced poly(lactic acid)/polycarbonate composites. J Appl Polym Sci 135:46881–46890

9. Seki M, Sato K, Yosomiya R (1992) Polyurethane elastomer-LiClO$_4$ complexes as a polymeric solid electrolyte. Macro Chem Phys 193:2971–2980

10. Vanheumen JD, Stevens JR (1995) The role of lithium salts in the conductivity and phase morphology of a thermoplastic polyurethane. Macromolecules 28:4268–4277

11. Kuo HH, Chen WC, Wen TC, Gopalan A (2002) A novel composite gel polymer electrolyte for rechargeable lithium batteries. J Power Sources 110:27–33

12. Du YL, Wen TC (2001) The feasibility study of composite electrolytes comprising thermoplastic polyurethane and poly(ethylene oxide). Mater Chem Phys 71:62–69

13. Santhosh P, Vasudevan T, Gopalan A, Lee KP (2006) Preparation and characterization of polyurethane/poly(vinylidene fluoride) composites and evaluation as polymer electrolytes. Mater Sci Eng B 135:65–73

14. Long J, Liu B, Zhang J (2009) Properties of poly(lactic acid)/poly(butylene adipate-co-terephthalate)/nanoparticle ternary composites. Ind Eng Chem Res 48:7594–7602

15. Han JJ, Huang HX (2011) Preparation and characterization of biodegradable polylactide/thermoplastic polyurethane elastomer blends. J Appl Polym Sci 120:3217–3223

16. Feng F, Ye L (2011) Morphologies and mechanical properties of polylactide/thermoplastic polyurethane elastomer blends. J Appl Polym Sci 119:2778–2783

17. Li Y, Shimizu H (2007) Toughening of polylactide by melt blending with a biodegradable poly(ether)urethane elastomer. Macromol Biosci 7:921–928

18. Pachon EYG, Graziano RV, Campos RM (2014) Structure of poly(lactic-acid) PLA nanofibers scaffolds prepared by electrospinning. IOP Conf Series Mat Sci Eng 59:012003

19. Touny AH, Bhaduri SB (2010) A reactive electrospinning approach for nanoporous PLA/monetite nanocomposite fibers. Mater Sci Eng C 30:1304–1312

20. Huang C, Thomas NL (2018) Fabricating porous poly(lactic acid) fibres via electrospinning. EurPolym J 99:464–476

21. Lee K, Lee B, Kim C, Kim H, Kim K, Nah C (2005) Stress-strain behavior of the electrospun thermoplastic polyurethane elastomer fiber mats. Macromol Res 13:441–445

22. Lee S, Obendorf S (2007) Use of electrospun nanofiber web for protective textile materials as barriers to liquid penetration. Textile Res J 77:696–702

23. Yuryev Y, Mohanty AK, Misra M (2017) Novel biocomposites from biobased PC/PLA blend matrix system for durable applications. Compos B 130:158–166

24. Schiffman JD, Schauer CL (2007) Cross-linking chitosan nanofibers. Biomacromol 8:594–601

25. Zhao YY, Yang QB, Lu XF, Wang C, Wei Y (2005) Study on correlation of morphology of electrospun products of polyacrylamide with ultrahigh molecular weight. J Polym Sci B 43:2190–2195

26. Xu J, Zhang J, Gao W, Liang H, Wang H, Li J (2009) Preparation of chitosan/PLA blend micro/nanofibers by electrospinning. Mater Lett 63:658–660

27. Pradhan KC, Nayak PL (2012) Synthesis and characterization of polyurethane nanocomposite from castor oil- hexamethylene diisocyanate (HMDI). Adv Appl Sci Res 5:3045–3052

28. Raja M, Ryu SH, Shanmugharaj AM (2013) Thermal, mechanical and electroactive shape memory properties of polyurethane (PU)/poly (lactic acid) (PLA)/CNT nanocomposites. Eur Polym J 49:3492–3500

29. Silva GG, Calado HDR, Musumeci AW, Martens W, Waclawik ER (2006) Polymer nanocomposites based on P3OT, TPU and SWNT: preparation and characterization. Int Conf Nanosc Nanotech 2006 IEEE, https://doi.org/10.1109/ICONN.2006.340581

30. Deshmukh KA, Khajanji P, Chopra S, Deshmukh A, Peshwe DR (2020) The influence of micro-graphite addition on nucleation efficiency and isothermal crystallization kinetics of thermoplastic polyurethane (TPU). Mater Today Proc 28:642–650

31. Lostocco MR, Huang SJ (1998) The hydrolysis of poly(lactic acid)/poly(hexamethylene succinate) blends. Poly Degrad Stabil 61:225–230

32. Ploypetchara N, Suppakula P, Atong D, Pechyena C (2014) Blend of polypropylene/poly(lactic acid) for medical packaging application: physicochemical, thermal, mechanical, and barrier properties. Energy Procedi 56:201–210

33. Yuan Y, Ruckenstein E (1998) Polyurethane toughened polylactide. Polym Bull 40:485–490

34. Lai SM, Lan YC (2013) Shape memory properties of melt-blended polylactic acid(PLA)/thermoplastic polyurethane (TPU) bio-based blends. J Polym Res 20:140–148

35. Trovati G, Sanches EA, Neto SC, Mascarenhas YP, Chiericet GO (2010) Characterization of polyurethane resins by FTIR, TGA and XRD. Inc J Appl Polym Sci 115:263–268